fluids

MDPI

Article

Transient Electrophoresis in Suspensions of Charged Porous Particles

Wei Z. Chen and Huan J. Keh *

Department of Chemical Engineering, National Taiwan University, Taipei 10617, Taiwan; r12524128@ntu.edu.tw
* Correspondence: huan@ntu.edu.tw; Tel.: +886-2-33663048

Abstract

The start-up of electrophoretic motion in a suspension of uniformly charged, porous, spherical particles within an arbitrary electrolyte solution under a suddenly applied electric field is investigated. The unsteady Stokes/Brinkman equations, modified to include the electric body force, are solved for the fluid velocity field using a unit cell model to account for the particle-particle interactions. An explicit expression for the transient electrophoretic velocity of a porous particle in a unit cell is derived in the Laplace transform domain as a function of the key governing parameters. The transient electrophoretic velocity, when normalized by its steady-state counterpart, increases monotonically with both elapsed time and the ratio of particle radius to Debye length, with other parameters held constant. It generally increases with the ratio of particle radius to permeation length and with porosity, while decreasing monotonically with an increase in the particle-to-fluid density ratio. Similar to its steady-state value, the transient electrophoretic mobility of the suspension is typically a decreasing function of the particle volume fraction. However, under conditions of small elapsed time and large density ratio, the transient mobility may exhibit an initial increase with particle volume fraction.

Keywords: starting electrophoresis; creeping flow; porous sphere; particle interaction effect; arbitrary electric double layer

1. Introduction

When an electric field is applied to a charged particle suspended in an electrolyte solution, the particle undergoes electrophoresis while the surrounding counterions and co-ions migrate, thereby inducing fluid motion. Electrophoresis represents one of the most widely utilized experimental techniques and operational methods for the manipulation, transport, assembly, separation, and characterization of colloidal particles. Analytical expressions for the steady electrophoretic mobility of charged particles have previously been derived for several idealized models, including the hard sphere (impermeable to solvent and ions) [1–6], the porous sphere (permeable) [7–10], and the soft sphere (with a rigid core and a porous surface layer) [11–13]. Although the original theoretical framework of electrophoresis focused on steady-state motion, transient effects are equally significant, since alternating or pulsed electric fields are frequently employed in measurements and applications involving colloidal electrophoresis [14–21]. In particular, the time-dependent behavior of particle mobility plays an essential role in high-speed colloidal processes within the sub-millisecond range, including electrophoretic separations in biochip devices, and the use of short-duration pulsed fields to separate particle migration from background electroosmotic flow or to suppress thermal broadening [22].

Check for updates

Academic Editor: Jun Yao

Received: 1 December 2025
Revised: 24 December 2025
Accepted: 28 December 2025
Published: 30 December 2025

Copyright: © 2025 by the authors. Licensee MDPI, Basel, Switzerland. This article is an open access article distributed under the terms and conditions of the Creative Commons Attribution (CC BY) license.

Assuming the fluid within the electric double layer surrounding a charged particle instantaneously reaches its electroosmotic terminal velocity when a uniform electric field is imposed, Morrison derived a closed-form solution for the starting electrophoretic velocity of a hard sphere under the thin double layer condition ($\kappa a \to \infty$, with a being the particle radius and κ^{-1} the Debye length) [23]. Subsequently, the transient start-up electrophoresis of a hard sphere [24] and a soft sphere [25] with a thin yet finite double layer ($\kappa a \geq 10$) was analyzed approximately by considering the dynamic relaxation of electroosmotic flow in the double layer under a suddenly applied electric field. On the other hand, theoretical investigations extended to transient electrophoresis of hard spheres [26,27], hard cylinders [28], and porous spheres (without consideration of particle porosity and particle volume fraction) [29] with arbitrary values of κa but small zeta potentials or fixed-charge densities, in response to a step change in the applied field.

In both steady and transient electrophoresis, concentrated suspensions of particles are frequently encountered. To evaluate particle–particle interactions on mean mobility, the unit cell model has been widely applied [30–35]. This model represents a homogeneous dispersion as an assembly of identical spherical cells, each containing one central particle and the surrounding concentric shell of fluid, thereby reducing the many-body suspension problem to a tractable single-cell formulation. Comparisons between measured mobilities in suspensions of charged particles and predictions of the cell model have shown good agreement across wide ranges of κa values and particle concentrations [36].

By adopting the unit cell model, the transient electrophoretic behavior of a suspension of identical hard spheres was investigated, taking into account dynamic electroosmosis in thin but finite double layers ($\kappa a \geq 10$) following the sudden application of an electric field [37]. More recently, the transient electrophoretic response of hard-sphere suspensions with arbitrary κa but low zeta potential was also analyzed (with no effects of particle porosity and particle permeability) [38,39]. In this study, we present an analysis of the start-up electrophoresis of suspensions composed of charged porous spheres with arbitrary κa, particle porosity, particle permeability, particle volume fraction, and other relevant parameters under a suddenly imposed electric field. An explicit formula for the transient electrophoretic mobility of porous spheres is obtained in the Laplace transform domain.

2. Analysis

The starting electrophoresis in a homogeneous suspension of identical charged porous spheres in a bounded solution of arbitrary electrolytes is considered. At the time $t = 0$, a uniform electric field $E_\infty \mathbf{e}_z$ is suddenly applied and carries on hereafter, where $\mathbf{e}_z$ is the unit vector in the z direction. Consequently, the particles undergo electrophoretic motion with a transient velocity equal to $U(t)\mathbf{e}_z$ [knowing that $U(0) = 0$] to be determined. As shown in Figure 1, we utilize the unit cell model in which each particle of radius a is enclosed by a concentric shell of the electrolyte solution of outer radius b, and $\phi = (a/b)^3$ represents the particle volume fraction of the suspension. The origin of the spherical coordinates (r, θ, φ) is set at the particle center, and the problem for a unit cell is axially symmetric about the z-axis (which coincides with $\theta = 0$).

The fluid velocity $\mathbf{v}(r, \theta)$ (satisfying the continuity equation $\nabla \cdot \mathbf{v} = 0$) and hydrodynamic pressure $p(r, \theta)$ of the electrokinetic flow is governed by the modified transient Stokes/Brinkman equations [40],

$$[1 - h(r)(1 - \varepsilon_p)]\rho \frac{\partial \mathbf{v}}{\partial t} - \eta \nabla^2 \mathbf{v} + h(r) f \Big(\mathbf{v} - U\mathbf{e}_z) + \nabla p = \varepsilon \nabla^2 \psi \nabla \psi, \tag{1}$$

where $\psi(r, \theta)$, η, ρ, and ε are the electric potential, viscosity, mass density, and dielectric permittivity, respectively, of the fluid, ε_p and f are the porosity and hydrodynamic friction

coefficient per unit volume, respectively, of the particle, $h(r)$ is a step function equal to unity if $0 \le r \le a$ and zero if $a < r \le b$, and Poisson's equation is incorporated. Note that the effects of the porosity ε_p in Equation (1) was not considered in a previous analysis [29] on the starting electrophoretic motion of an isolated porous sphere. The steady-state electrophoretic velocity $U(t \to \infty) = U_\infty$, which does not directly depend on the porosity and density of the particle, is available in the literature [34,41].

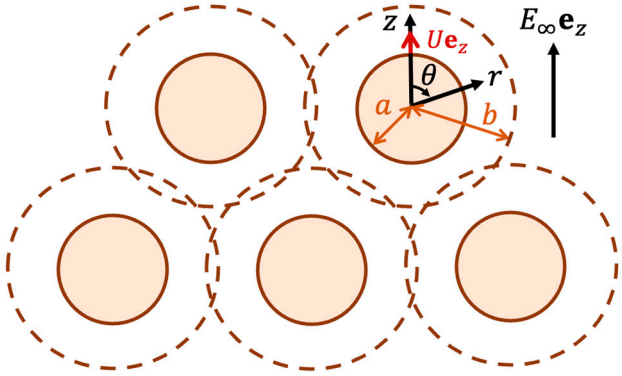


Figure 1. Geometric sketch of the cell model for the electrophoresis of a suspension of porous spherical particles.

The electrical potential profile ψ of the electrolyte solution in a unit cell can be expressed as the equilibrium potential profile $\psi_{eq}(r)$ caused by the fixed charge within the porous sphere and ambient diffuse ions, which is assumed to be relatively small, added to the potential profile induced by the applied electric field $E_\infty \mathbf{e}_z$,

$$\psi = \psi_{eq} - E_\infty r \cos\theta. \tag{2}$$

The equilibrium potential satisfying the linearized Poisson–Boltzmann equation (under the Debye–Hückel approximation) and appropriate boundary conditions of the uniformly charged porous sphere in the cell is [34]

$$\psi_{eq} = \frac{Q}{\varepsilon\kappa^2}\{1 - [(\kappa b - \kappa a)\cosh(\kappa b - \kappa a) + (\kappa^2 ab - 1)\sinh(\kappa b - \kappa a)]\frac{\sinh(\kappa r)}{\alpha(\kappa b)\kappa r}\} \text{ if } 0 \le r \le a, \tag{3}$$

$$\psi_{eq} = \frac{\alpha(\kappa a)Q}{\alpha(\kappa b)\varepsilon\kappa^3 r}[\kappa b\cosh(\kappa b - \kappa r) - \sinh(\kappa b - \kappa r)] \text{ if } a \le r \le b, \tag{4}$$

where

$$\alpha(x) = x\cosh x - \sinh x, \tag{5}$$

Q is the fixed-charge density within the porous sphere, which is assumed to be a constant, and κ is the reciprocal of the Debye length.

Taking the curl of Equation (1) after the substitution of Equation (2), we obtain

$$[1 - h(r)(1 - \varepsilon_p)]\frac{1}{\nu}\frac{\partial}{\partial t}\nabla \times \mathbf{v} - [\nabla^2 - h(r)\lambda^2]\nabla \times \mathbf{v} = -\frac{\varepsilon}{\eta}E_\infty \nabla \times (\mathbf{e}_z \nabla^2 \psi_{eq}), \tag{6}$$

where $\lambda^2 = f/\eta$ is the reciprocal of the fluid permeability in the porous particle and $\nu = \eta/\rho$ is the kinematic viscosity of the fluid. The nonvanishing components of $\mathbf{v}$ can be expressed in terms of the Stokes stream function Ψ, which immediately satisfies the continuity equation $\nabla \cdot \mathbf{v} = 0$,

$$v_r = -\frac{1}{r^2 \sin\theta}\frac{\partial \Psi}{\partial \theta}, \; v_\theta = \frac{1}{r\sin\theta}\frac{\partial \Psi}{\partial r}. \tag{7}$$

The application of Equation (7) to Equation (6) results in

$$E^2(E^2-\lambda^2-\frac{\varepsilon_p}{\nu}\frac{\partial}{\partial t})\Psi^{(i)}=-\frac{\varepsilon\kappa^2}{\eta}E_\infty r\frac{d\psi_{eq}}{dr}\sin^2\theta \qquad \text{if } 0\le r\le a, \tag{8}$$

$$E^2(E^2-\frac{1}{\nu}\frac{\partial}{\partial t})\Psi^{(o)}=-\frac{\varepsilon\kappa^2}{\eta}E_\infty r\frac{d\psi_{eq}}{dr}\sin^2\theta \qquad \text{if } a\le r\le b, \tag{9}$$

where the superscripts (i) and (o) represent the internal and external flows, respectively, and E^2 is the Stokes operator given by

$$E^2=\frac{\partial^2}{\partial r^2}+\frac{\sin\theta}{r^2}\frac{\partial}{\partial\theta}(\frac{1}{\sin\theta}\frac{\partial}{\partial\theta}). \tag{10}$$

The initial and boundary conditions of the flow field are

$$t=0:\ \mathbf{v}^{(i)}=\mathbf{v}^{(o)}=\mathbf{0}, \tag{11}$$

$$r=a:\mathbf{v}\text{ and }\boldsymbol{\tau}-p\mathbf{I}\text{ are continuous}, \tag{12}$$

$$r=b:v_r^{(o)}=0, \tag{13}$$

$$\tau_{r\theta}^{(o)}=\eta\{r\frac{\partial}{\partial r}[\frac{v_\theta^{(o)}}{r}]+\frac{1}{r}\frac{\partial v_r^{(o)}}{\partial\theta}\}=0\ (\text{fortheHappelmodel}), \tag{14}$$

$$\left[\nabla\times\mathbf{v}^{(o)}\right]_\varphi=\frac{1}{r}\frac{\partial}{\partial r}[rv_\theta^{(o)}]-\frac{1}{r}\frac{\partial v_r^{(o)}}{\partial\theta}=0\ (\text{fortheKuwabaramodel}), \tag{15}$$

where $\boldsymbol{\tau}=\eta[\nabla\mathbf{v}+(\nabla\mathbf{v})^T]$ is the deviatoric stress tensor and $\mathbf{I}$ is the unit tensor.

The internal and external stream functions can be expressed as

$$\Psi^{(i,o)}=g^{(i,o)}(r,t)\sin^2\theta. \tag{16}$$

In terms of the Laplace transform (with a bar over the variable); Equations (8) and (9) with the substitution of Equation (16) can be expressed as

$$(\frac{d^2}{dr^2}-\frac{2}{r^2})(\frac{d^2}{dr^2}-\frac{2}{r^2}-\lambda^2-\frac{\varepsilon_p s}{\nu})\bar{g}^{(i)}(r,s)=\frac{r}{s}G(r), \tag{17}$$

$$(\frac{d^2}{dr^2}-\frac{2}{r^2})(\frac{d^2}{dr^2}-\frac{2}{r^2}-\frac{s}{\nu})\bar{g}^{(o)}(r,s)=\frac{r}{s}G(r), \tag{18}$$

where s is the transform parameter and

$$G(r)=-\frac{\varepsilon}{\eta}\kappa^2E_\infty\frac{d\psi_{eq}}{dr}. \tag{19}$$

The general solution of Equations (8) and (9) or Equations (17) and (18) that satisfies the initial condition in Equation (11) is

$$\bar{\Psi}^{(i)}=\{[C_1(\frac{r}{a})^3+C_2+C_3\alpha(Br)+C_4\beta(Br)]\frac{a}{r}+\bar{g}_p^{(i)}(r,s)\}\sin^2\theta\ \text{ if } 0\le r\le a, \tag{20}$$

$$\bar{\Psi}^{(o)}=\{[C_5(\frac{r}{a})^3+C_6+C_7\gamma(Ar)+C_8\gamma(-Ar)]\frac{a}{r}+\bar{g}_p^{(o)}(r,s)\}\sin^2\theta\ \text{ if } a\le r\le b, \tag{21}$$

with the particular solution

$$\bar{g}_p^{(i)}=\frac{1}{3B^2sr}[J_3(r)-r^3J_0(r)]-\frac{1}{B^5sr}[\alpha(Br)I_\beta(r)-\beta(Br)I_\alpha(r)], \tag{22}$$

$$\overline{g}_{\mathrm{p}}^{(\mathrm{o})} = \frac{1}{3A^2sr}[J_3(r) - r^3 J_0(r)] - \frac{1}{2A^5sr}[\gamma(Ar)I_{\gamma-}(r) - \gamma(-Ar)I_{\gamma+}(r)], \tag{23}$$

where

$$\beta(x) = x\sinh x - \cosh x, \tag{24}$$

$$\gamma(x) = (1-x)\mathrm{e}^x, \tag{25}$$

$$J_n(r) = \int_a^r r^n G(r)\mathrm{d}r, \tag{26}$$

$$I_\alpha(r) = \int_a^r \alpha(Br)G(r)\mathrm{d}r, \tag{27}$$

$$I_\beta(r) = \int_a^r \beta(Br)G(r)\mathrm{d}r, \tag{28}$$

$$I_{\gamma\pm}(r) = \int_a^r \gamma(\pm Ar)G(r)\mathrm{d}r, \tag{29}$$

$A = \sqrt{s/\nu}$, and $B = \sqrt{\lambda^2 + \varepsilon_{\mathrm{p}} s/\nu}$.

The unknown constants $C_1 \sim C_8$ in Equations (20) and (21) can be derived from the boundary conditions in Equations (12)–(15) and expressed as follows:

$$C_1 = M_1 a^2 \overline{U} + M_2 a^3, \tag{30}$$

$$C_2 = -\frac{J_3(0)}{3saB^2}, \tag{31}$$

$$C_3 = M_3 a^2 \overline{U} + M_4 a^3, \tag{32}$$

$$C_4 = -\frac{I_\alpha(0)}{saB^5}, \tag{33}$$

$$C_5 = M_5 a^2 \overline{U} + M_6 a^3, \tag{34}$$

$$C_6 = M_7 a^2 \overline{U} + M_8 a^3, \tag{35}$$

$$C_7 = M_9 a^2 \overline{U} + M_{10} a^3, \tag{36}$$

$$C_8 = M_{11} a^2 \overline{U} + M_{12} a^3, \tag{37}$$

where the dimensionless coefficients $M_1 \sim M_{12}$ are lengthy functions of related parameters that can be provided on request.

The substitution of Equations (20) and (30)–(33) into Equation (7) yields the Laplace transform of the fluid velocity inside the porous sphere,

$$\overline{v}_r^{(\mathrm{i})} = -F(r)\cos\theta, \tag{38}$$

$$\overline{v}_\theta^{(\mathrm{i})} = \frac{\partial}{2r\partial r}[r^2 F(r)]\sin\theta, \tag{39}$$

where

$$F(r) = \frac{2a}{r^3}[C_1(\frac{r}{a})^3 + C_2 + C_3\alpha(Br) + C_4\beta(Br)] + \frac{2}{3B^2r^3s}[J_3(r) - r^3 J_0(r)] + \frac{2}{B^5r^3s}[\beta(Br)I_\alpha(r) - \alpha(Br)I_\beta(r)]. \tag{40}$$

The electrostatic force acting on the porous sphere is

$$F_{\mathrm{e}} = \frac{4}{3}\pi a^3 Q E_\infty, \tag{41}$$

in the z direction. The hydrodynamic force acting on the porous sphere is

$$F_{\mathrm{h}} = 2\pi \int_0^{\pi} \int_0^{a} \mathbf{e}_z \cdot f(\mathbf{v}^{(\mathrm{i})} - U\mathbf{e}_z) r^2 \sin\theta \mathrm{d}r\mathrm{d}\theta, \tag{42}$$

which is also in the z direction, dependent on the friction coefficient $f = \eta\lambda^2$, and opposite to F_{e} in sign. Substituting Equations (38) and (39) into Equation (42), we obtain

$$\overline{F}_{\mathrm{h}} = -\frac{4}{3}\pi a^3 \eta \lambda^2 [F(a) + \overline{U}]. \tag{43}$$

The summation of the electric force and hydrodynamic force is equal to the product of the mass and acceleration of the particle:

$$F_{\mathrm{e}} + F_{\mathrm{h}} = \frac{4}{3}\pi a^3 (1 - \varepsilon_{\mathrm{p}}) \rho_{\mathrm{p}} \frac{\mathrm{d}U}{\mathrm{d}t,} \tag{44}$$

where ρ_{p} is the mass density of the solid fragment of the porous particle. Taking the Laplace transform of Equation (44) and substituting Equations (41) and (43) into it, we obtain a transformed equation for the response of electrophoresis to a suddenly applied electric field,

$$\overline{U} = \frac{1}{3sB^5a^3}\{\eta\lambda^2[1 + 2M_1 + 2\alpha(Ba)M_3] + s(1 - \varepsilon_{\mathrm{p}})\rho_{\mathrm{P}}\}^{-1} \times [3B^5a^3 Q E_\infty + 2\eta\lambda^2\{B^3 J_3(0) + 3\beta(aB) I_\alpha(0) - 3sB^5a^4[M_2 + \alpha(aB)M_4]\}]. \tag{45}$$

The particle's transient velocity U can be obtained by numerical inverse Laplace transform [42,43] of Equation (45).

3. Results and Discussion

For the case of a single charged porous sphere [$\varphi = (a/b)^3 = 0$] at maximum porosity ($\varepsilon_{\mathrm{p}} = 1$), the transient electrophoretic velocity U, normalized by the terminal electrophoretic velocity U_∞ [7] was obtained using the numerical inverse transform of a simplified form of Equation (45) for various values of the dimensionless elapsed time $\nu t/a^2$, the ratio of particle radius to Debye length κa, the ratio of particle radius to permeation length λa, and the particle-to-fluid density ratio ρ_{p}/ρ [29]. The normalized electrophoretic velocity U/U_∞ was found to increase monotonically with $\nu t/a^2$ (developing continuously from zero at $t = 0$ to unity as $t \to \infty$) and with κa, but to decrease monotonically with ρ_{p}/ρ (developing more slowly for heavier particles and vanishing in the limit $\rho_{\mathrm{p}}/\rho \to \infty$), keeping all other parameters fixed. Moreover, U/U_∞ generally rises with increasing λa (or decreasing permeability of the porous sphere) for given values of $\nu t/a^2$, κa, and ρ_{p}/ρ, though it may decline again once λa becomes relatively large. The results of the transient electrophoretic velocity obtained in the present work under the same conditions ($\varphi = 0$ and $\varepsilon_{\mathrm{p}} = 1$) agree very well with these previous results [29] of a single charged porous sphere at maximum porosity.

The normalized electrophoretic velocity U/U_∞ of a single charged porous sphere with various values of the porosity ε_{p} is shown in Figures 2–5 as a function of the parameters $\nu t/a^2$, λa, κa, and ρ_{p}/ρ, respectively. These results reveal that U/U_∞ typically increases with ε_{p} from $\varepsilon_{\mathrm{p}} \to 0$ (the particle is essentially impermeable) to $\varepsilon_{\mathrm{p}} \to 1$, indicating that particles of lower porosity exhibit longer relaxation times and lag behind particles of higher porosity in the buildup of electrophoretic velocity. On the other hand, the normalized sedimentation velocity of the porous sphere may slightly decrease with an increase in ε_{p} when the value of ρ_{p}/ρ is relatively small [40]. For finite ε_{p}, Figures 2–5 further demonstrate that U/U_∞ develops steadily with time from zero at $t = 0$ to unity as $t \to \infty$, generally increases with λa to a maximum before falling with further increases in λa, increases

monotonically with κa, and decreases monotonically with ρ_p/ρ. However, the normalized sedimentation velocity decreases monotonically with an increase in λa [40].

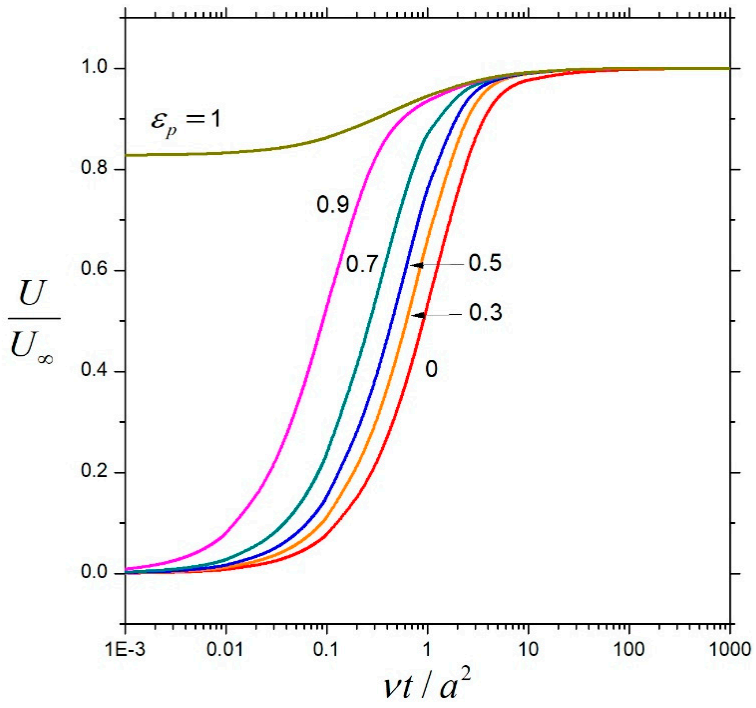


Figure 2. Normalized electrophoretic velocity U/U_∞ versus the dimensionless time $\nu t/a^2$ with $\rho_P/\rho = 1$, $\kappa a = 0.1$, $\lambda a = 1$, and ε_P as a parameter.

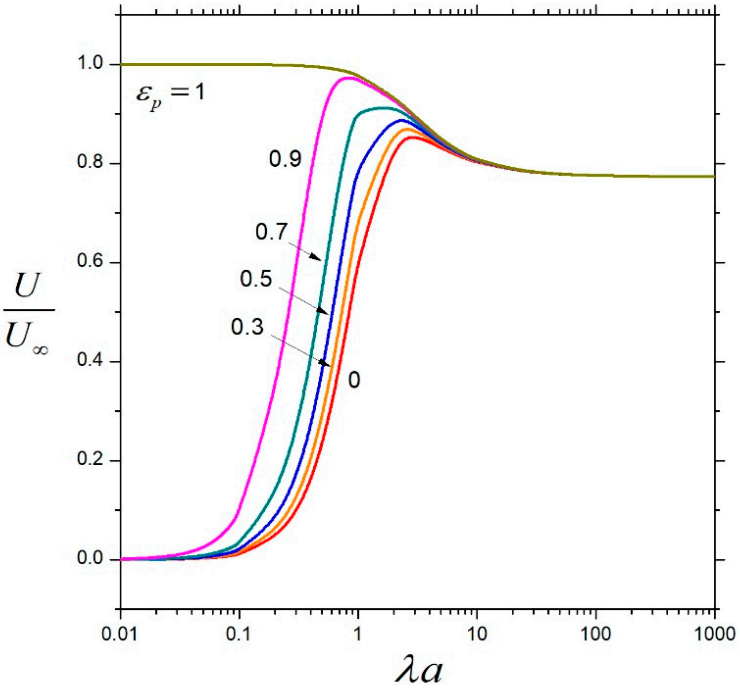


Figure 3. Normalized electrophoretic velocity U/U_∞ versus the ratio of particle radius to permeation length λa with $\nu t/a^2 = 1$, $\rho_P/\rho = 1$, $\kappa a = 1$, and ε_P as a parameter.

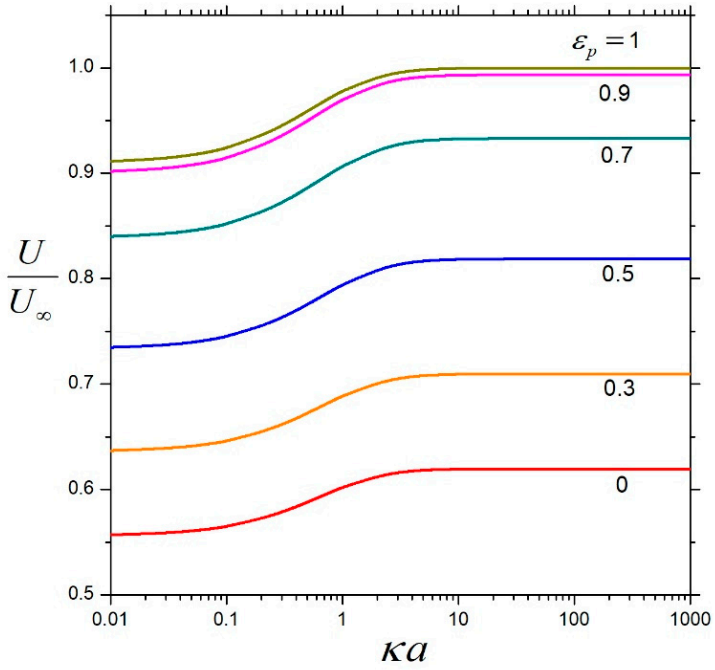


Figure 4. Normalized electrophoretic velocity U/U_∞ versus the ratio of particle radius to Debye length κa with $\nu t/a^2 = 1$, $\rho_P/\rho = 1$, $\lambda a = 1$, and ε_P as a parameter.

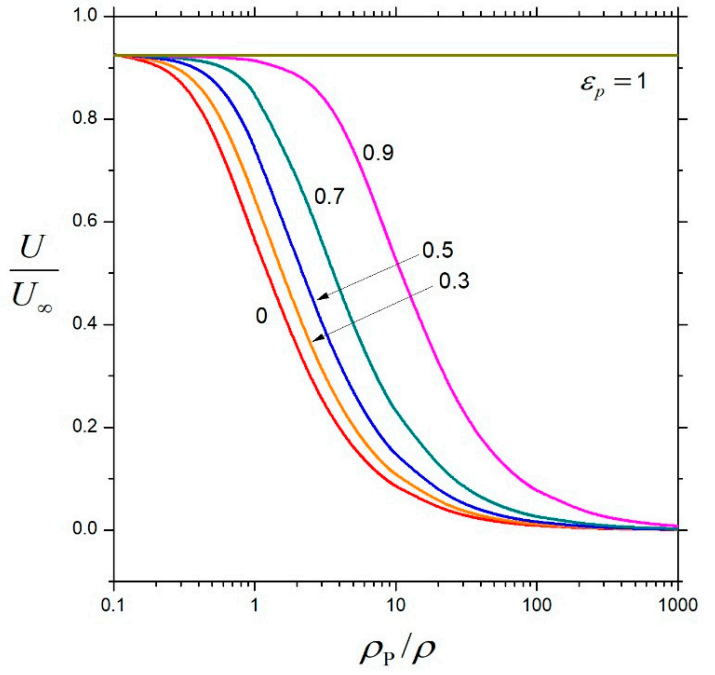


Figure 5. Normalized electrophoretic velocity U/U_∞ versus the particle-to-fluid density ratio ρ_P/ρ with $\nu t/a^2 = 1$, $\kappa a = 0.1$, $\lambda a = 1$, and ε_P as a parameter.

The results for the dimensionless starting electrophoretic velocity $\eta U/a^2 Q E_\infty$ of porous spheres with constant fixed-charge density Q in a suspension, obtained from numerical inverse transforms of Equation (45) for both Happel and Kuwabara cell models, are plotted against the dimensionless time $\nu t/a^2$ in Figures 6–8 for various values of the particle volume fraction φ, the ratio of particle radius to permeation length λa, and the porosity ε_P, respectively. In contrast, this dimensionless velocity is plotted against the particle volume fraction φ in Figures 9 and 10 for various values of the particle-to-fluid density ratio ρ_P/ρ and the ratio of particle radius to Debye length κa, respectively. The

data are shown up to $\varphi = 0.74$, which represents the maximum achievable packing for a collection of identical spheres [30]. The steady electrophoretic velocity $\eta U_\infty / a^2 Q E_\infty$ is independent of ε_p and ρ_p/ρ, and is generally a decreasing function of φ, consistent with published findings [34,41]. The effect of φ and other relevant parameters on the time evolution of $\eta U / a^2 Q E_\infty$ are significant.

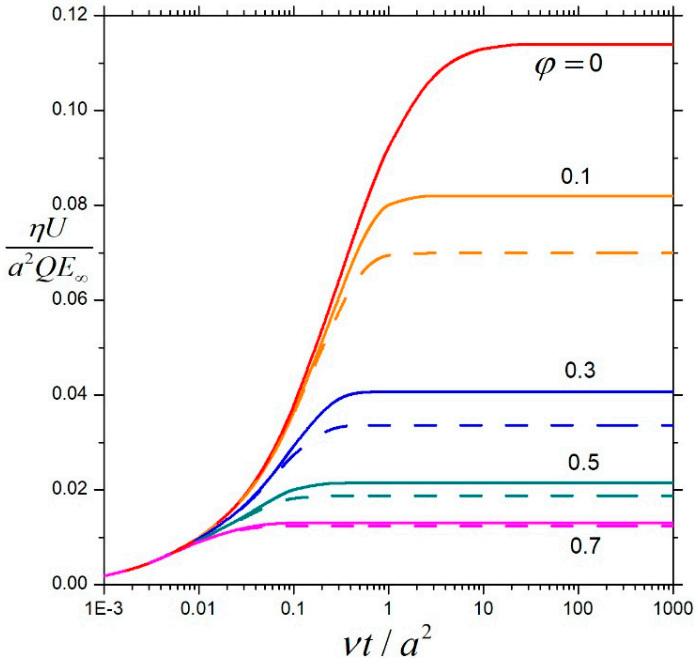


Figure 6. Dimensionless electrophoretic velocity $\eta U / a^2 Q E_\infty$ versus $\nu t / a^2$ with $\rho_P/\rho = 1$, $\varepsilon_P = 0.5$, $\kappa a = 1$, $\lambda a = 10$, and φ as a parameter. The solid and dashed curves represent the Happel and Kuwabara models, respectively.

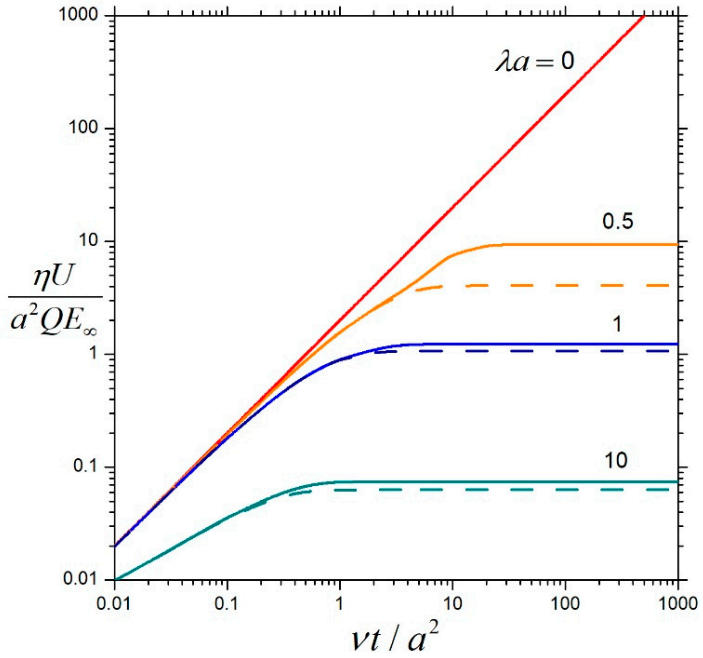


Figure 7. Dimensionless electrophoretic velocity $\eta U / a^2 Q E_\infty$ versus $\nu t / a^2$ with $\varphi = 0.125$, $\rho_P/\rho = 1$, $\varepsilon_P = 0.5$, $\kappa a = 1$, and λa as a parameter. The solid and dashed curves represent the Happel and Kuwabara models, respectively.

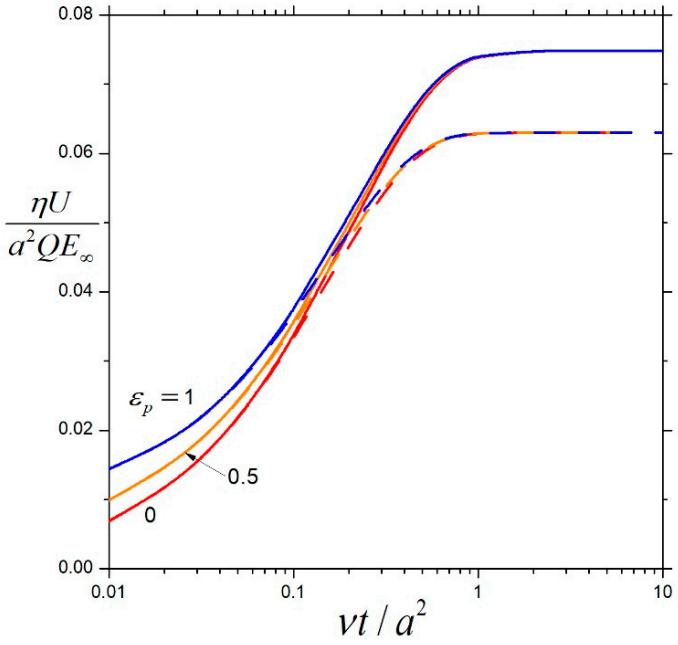


Figure 8. Dimensionless electrophoretic velocity $\eta U/a^2 Q E_\infty$ versus $\nu t/a^2$ with $\varphi = 0.125$, $\rho_P/\rho = 1$, $\kappa a = 1$, $\lambda a = 10$, and ε_P as a parameter. The solid and dashed curves represent the Happel and Kuwabara models, respectively.

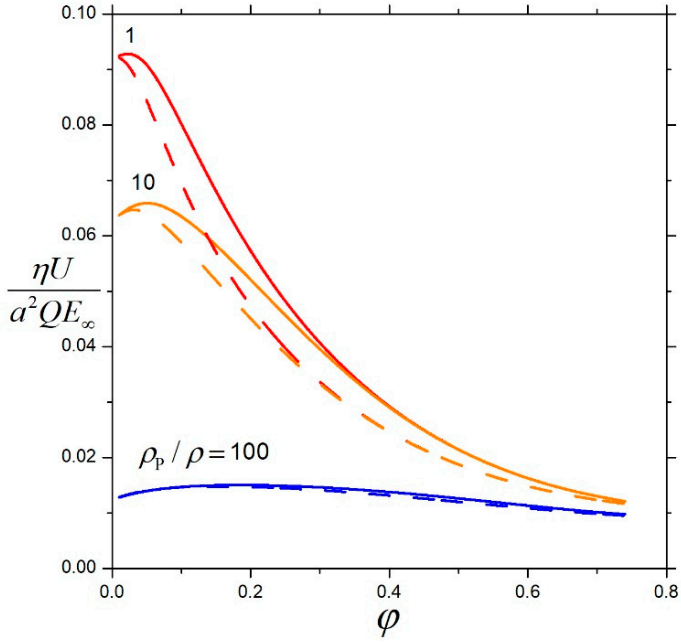


Figure 9. Dimensionless electrophoretic velocity $\eta U/a^2 Q E_\infty$ versus φ with $\nu t/a^2 = 1$, $\varepsilon_P = 0.5$, $\kappa a = 1$, $\lambda a = 10$, and ρ_P/ρ as a parameter. The solid and dashed curves represent the Happel and Kuwabara models, respectively.

For given $\nu t/a^2$, ρ_p/ρ, ε_p, and φ, as in Figures 7 and 10, the transient electrophoretic velocity $\eta U/a^2 Q E_\infty$ (non-dimensionlized with the chosen length scale a) decreases with increasing λa and κa, in the same manner as the steady velocity $\eta U_\infty/a^2 Q E_\infty$ [41]. Furthermore, as in Figure 8, $\eta U/a^2 Q E_\infty$ increases with increasing ε_p from $\varepsilon_p \to 0$ to $\varepsilon_p \to 1$, holding other parameters constant. For given $\nu t/a^2$, ρ_p/ρ, κa, λa, and ε_p, the transient velocity $\eta U/a^2 Q E_\infty$ generally decreases with φ, as seen in Figure 6 and at steady state, though it may increase with φ when $\nu t/a^2$ is small, ρ_p/ρ is large, and φ is small, as in Figures 9 and 10. For all combinations of $\nu t/a^2$, ρ_p/ρ, κa, λa, ε_p, and φ, as illustrated in

Figures 6–10, the Kuwabara cell model predicts smaller values of $\eta U/a^2QE_\infty$ than the Happel model, because the zero-vorticity condition in the Kuwabara model induces greater energy dissipation in the cell than particle drag alone due to the added stress at the outer cell boundary [44], but the discrepancies are generally negligible. The dependence of the dimensionless transient electrophoretic velocity $\eta U/a^2QE_\infty$ on the parameters $\nu t/a^2$, ρ_p/ρ, κa, and φ shown in the present work is consistent with that of the dimensionless transient electrophoretic velocity $\eta U/a\sigma E_\infty$ on these parameters [38] for a suspension of hard spheres with constant surface charge density σ.

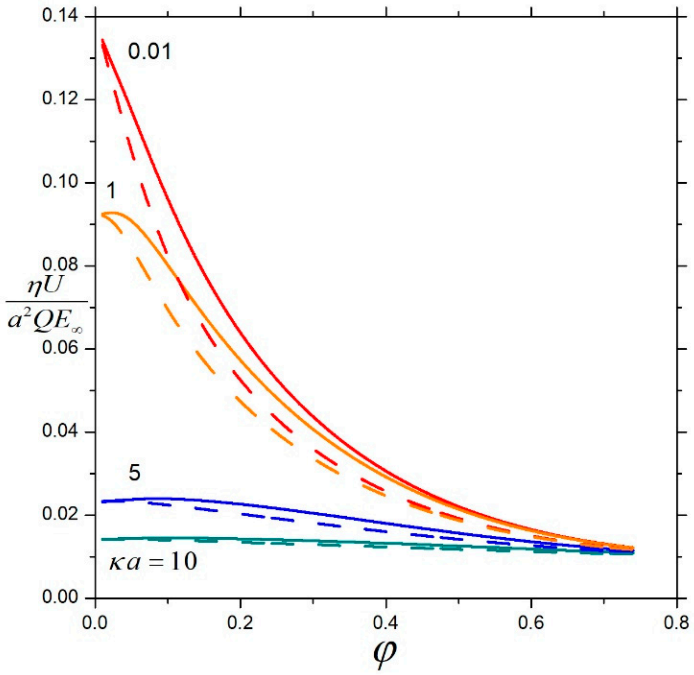


Figure 10. Dimensionless electrophoretic velocity $\eta U/a^2QE_\infty$ versus φ with $\nu t/a^2 = 1$, $\rho_P/\rho = 1$, $\varepsilon_P = 0.5$, $\lambda a = 10$, and κa as a parameter. The solid and dashed curves represent the Happel and Kuwabara models, respectively.

4. Conclusions

In this work, the starting electrophoretic motion in a suspension of uniformly charged, porous, spherical particles within an arbitrary electrolyte solution caused by the sudden application of an electric field is analyzed. The unsteady Stokes/Brinkman equations, modified to include the electric force, are solved using a unit cell model. An explicit formula for the transient electrophoretic velocity of the porous particle in a unit cell is obtained in the Laplace transform domain as a function of related parameters. The transient electrophoretic velocity normalized by its steady-state value increases monotonically with increases in the scaled elapsed time $\nu t/a^2$ and the ratio of particle radius to Debye length κa, generally increases with increases in the ratio of particle radius to permeation length λa and the porosity ε_p, but decreases monotonically with an increase in the particle-to-fluid density ratio ρ_p/ρ, with other parameters held constant. Similar to its steady-state value, the transient electrophoretic mobility is generally a decreasing function of the particle volume fraction φ of the suspension, but it may exhibit an initial increase with φ when $\nu t/a^2$ is small and ρ_p/ρ is large.

Author Contributions: Conceptualization, H.J.K.; methodology, H.J.K. and W.Z.C.; investigation, H.J.K. and W.Z.C.; writing—original draft preparation, H.J.K. and W.Z.C.; writing—review and editing, H.J.K.; supervision, H.J.K.; funding acquisition, H.J.K. All authors have read and agreed to the published version of the manuscript.

Funding: This research was funded by the National Science and Technology Council, Taiwan (Republic of China), grant number NSTC113-2221-E-002-063-MY2.

Data Availability Statement: Data is contained within the article.

Conflicts of Interest: The authors declare no conflicts of interest. The funders had no role in the design of the study; in the collection, analyses, or interpretation of data; in the writing of the manuscript; or in the decision to publish the results.

References

1. Henry, D.C. The Cataphoresis of Suspended Particles. Part I.—The Equation of Cataphoresis. *Proc. R. Soc. Lond. Ser. A* **1931**, *133*, 106–129.
2. Morrison, F.A. Electrophoresis of a Particle of Arbitrary Shape. *J. Colloid Interface Sci.* **1970**, *34*, 210–214. [CrossRef]
3. Dukhin, S.S.; Derjaguin, B.V. *Surface and Colloid Science*; Matijevic, E., Ed.; Wiley: New York, NY, USA, 1974; Volume 7.
4. O'Brien, R.W.; White, L.R. Electrophoretic Mobility of a Spherical Colloidal Particle. *J. Chem. Soc. Faraday Trans. 2* **1978**, *74*, 1607–1626. [CrossRef]
5. Ohshima, H.; Healy, T.W.; White, L.R. Approximate Analytic Expressions for the Electrophoretic Mobility of Spherical Colloidal Particles and the Conductivity of Their Dilute Suspensions. *J. Chem. Soc. Faraday Trans. 2* **1983**, *79*, 1613–1628. [CrossRef]
6. O'Brien, R.W. The Solution of the Electrokinetic Equations for Colloidal Particles with Thin Double Layers. *J. Colloid Interface Sci.* **1983**, *92*, 204–216. [CrossRef]
7. Hermans, J.J.; Fujita, H. Electrophoresis of Charged Polymer Molecules with Partial Free Drainage. *Koninkl. Ned. Akad. Wetenschap. Proc. Ser. B* **1955**, *58*, 182–187.
8. Gopmandal, P.P.; Bhattacharyya, S.; Barman, B. Effect of Induced Electric Field on Migration of a Charged Porous Particle. *Eur. Phys. J. E* **2014**, *37*, 104. [CrossRef]
9. Huang, H.Y.; Keh, H.J. Electrophoretic Mobility and Electric Conductivity in Suspensions of Charge-Regulating Porous Particles. *Colloid Polym. Sci.* **2015**, *293*, 1903–1914. [CrossRef]
10. Majee, P.S.; Bhattacharyya, S.; Dutta, P. On Electrophoresis of a pH-Regulated Nanogel with Ion Partitioning Effects. *Electrophoresis* **2019**, *40*, 699–709. [CrossRef]
11. Duval, J.F.L.; Ohshima, H. Electrophoresis of Diffuse Soft Particles. *Langmuir* **2006**, *22*, 3533–3546. [CrossRef] [PubMed]
12. Liu, H.C.; Keh, H.J. Electrophoresis and Electric Conduction in a Suspension of Charged Soft Spheres. *Colloid Polym. Sci.* **2016**, *294*, 1129–1141. [CrossRef]
13. Maurya, S.K.; Gopmandal, P.P.; Ohshima, H.; Duval, J.F.L. Electrophoresis of Composite Soft Particles with Differentiated Core and Shell Permeabilities to Ions and Fluid Flow. *J. Colloid Interface Sci.* **2020**, *558*, 280–290. [CrossRef]
14. Ivory, C.F. Transient Electrophoresis of a Dielectric Sphere. *J. Colloid Interface Sci.* **1984**, *100*, 239–249. [CrossRef]
15. Rasmusson, M.; Akerman, B. Dynamic Mobility of DNA. *Langmuir* **1998**, *14*, 3512–3516. [CrossRef]
16. Ahualli, S.; Jimenez, M.L.; Carrique, F.; Delgado, A.V. AC Electrokinetics of Concentrated Suspensions of Soft Particles. *Langmuir* **2009**, *25*, 1986–1997. [CrossRef] [PubMed]
17. Ammam, M.; Fransaer, J. AC-Electrophoretic Deposition of Glucose Oxidase. *Biosens. Bioelectron.* **2009**, *25*, 191–197. [CrossRef]
18. Khair, A.S. Transient Phoretic Migration of a Permselective Colloidal Particle. *J. Colloid Interface Sci.* **2012**, *381*, 183–188. [CrossRef]
19. Neirinck, B.; Van der Biest, O.; Vleugels, J. A Current Opinion on Electrophoretic Deposition in Pulsed and Alternating Fields. *J. Phys. Chem. B* **2013**, *117*, 1516–1526. [CrossRef]
20. Carrique, F.; Ruiz-Reina, E.; Roa, R.; Arroyo, F.J.; Delgado, A.V. Ionic Coupling Effects in Dynamic Electrophoresis and Electric Permittivity of Aqueous Concentrated Suspensions. *Colloids Surf. A* **2018**, *541*, 195–211. [CrossRef]
21. Ohshima, H. Transient Dynamic Electrophoresis of a Soft Particle. *Electrophoresis* **2024**, *45*, 2087–2094. [CrossRef] [PubMed]
22. Yossifon, G.; Frankel, I.; Miloh, T. Macro-scale Description of Transient Electro-kinetic Phenomena over Polarizable Dielectric Solids. *J. Fluid Mech.* **2009**, *620*, 241–262. [CrossRef]
23. Morrison, F.A. Transient Electrophoresis of a Dielectric Sphere. *J. Colloid Interface Sci.* **1969**, *29*, 687–691. [CrossRef]
24. Keh, H.J.; Huang, Y.C. Transient Electrophoresis of Dielectric Spheres. *J. Colloid Interface Sci.* **2005**, *291*, 282–291. [CrossRef]
25. Ohshima, H. Transient Electrophoresis of a Spherical Soft Particle. *Colloid Polym. Sci.* **2022**, *300*, 1369–1377. [CrossRef]
26. Huang, Y.C.; Keh, H.J. Transient Electrophoresis of Spherical Particles at Low Potential and Arbitrary Double-Layer Thickness. *Langmuir* **2005**, *21*, 11659–11665. [CrossRef] [PubMed]
27. Sherief, H.H.; Faltas, M.S.; Ragab, K.E. Transient Electrophoresis of a Conducting Spherical Particle Embedded in an Electrolyte-Saturated Brinkman Medium. *Electrophoresis* **2021**, *42*, 1636–1647. [CrossRef] [PubMed]
28. Ayman, M.; Saad, E.I.; Faltas, M.S. Transient Electrophoresis of a Conducting Cylindrical Colloidal Particle Suspended in a Brinkman Medium. *Z. Angew. Math. Phys.* **2024**, *75*, 53. [CrossRef]
29. Lai, Y.C.; Keh, H.J. Transient Electrophoresis of a Charged Porous Particle. *Electrophoresis* **2020**, *41*, 259–265. [CrossRef]

30. Levine, S.; Neale, G.H. The Prediction of Electrokinetic Phenomena within Multiparticle Systems I. Electrophoresis and Electroosmosis. *J. Colloid Interface Sci.* **1974**, *47*, 520–529. [CrossRef]
31. Zharkikh, N.I.; Shilov, V.N. Theory of Collective Electrophoresis of Spherical Particles in the Henry Approximation. *Colloid J. USSR* **1982**, *43*, 865–870.
32. Carrique, F.; Cuquejo, J.; Arroyo, F.J.; Jimenez, M.L.; Delgado, Á.V. Influence of Cell-Model Boundary Conditions on the Conductivity and Electrophoretic Mobility of Concentrated Suspensions. *Adv. Colloid Interface Sci.* **2005**, *118*, 43–50. [CrossRef]
33. Zholkovskij, E.K.; Masliyah, J.H.; Shilov, V.N.; Bhattacharjee, S. Electrokinetic Phenomena in Concentrated Disperse Systems: General Problem Formulation and Spherical Cell Approach. *Adv. Colloid Interface Sci.* **2007**, *134–135*, 279–321. [CrossRef] [PubMed]
34. Keh, H.J.; Liu, C.P. Electric Conductivity and Electrophoretic Mobility in Suspensions of Charged Porous Spheres. *J. Phys. Chem. C* **2010**, *114*, 22044–22054. [CrossRef]
35. Saad, E.I. Time-varying Brinkman Electrophoresis of a Charged Cylinder-in-Cell Model. *Eur. J. Mech. B Fluids* **2020**, *79*, 357–366. [CrossRef]
36. Miller, N.P.; Berg, J.C. Experiments on the Electrophoresis of Porous Aggregates. *J. Colloid Interface Sci.* **1993**, *159*, 253–254. [CrossRef]
37. Chiang, C.C.; Keh, H.J. Startup of Electrophoresis in a Suspension of Colloidal Spheres. *Electrophoresis* **2015**, *36*, 3002–3008. [CrossRef]
38. Lai, Y.C.; Keh, H.J. Transient Electrophoresis in a Suspension of Charged Particles with Arbitrary Electric Double Layers. *Electrophoresis* **2021**, *42*, 2126–2133. [CrossRef]
39. Ohshima, H. Transient Electrophoresis of Spherical Colloidal Particles in a Multi-particle Suspension. *Colloid Polym. Sci.* **2024**, *302*, 1407–1413. [CrossRef]
40. Yu, C.W.; Keh, H.J. Transient Slow Motion of a Porous Sphere. *Fluid Dyn. Res.* **2024**, *56*, 015503. [CrossRef]
41. Huang, H.Y.; Keh, H.J. Diffusiophoresis in Suspensions of Charged Porous Particles. *J. Phys. Chem. B* **2015**, *119*, 2040–2050. [CrossRef] [PubMed]
42. Talbot, A. The Accurate Numerical Inversion of Laplace Transforms. *J. Inst. Maths. Applics.* **1979**, *23*, 97–120. [CrossRef]
43. Murli, A.; Rizzardi, M. Talbot's Method for the Laplace Inversion Problem. *ACM Trans. Math. Softw.* **1990**, *16*, 158–168. [CrossRef]
44. Happel, J.; Brenner, H. *Low Reynolds Number Hydrodynamics*; Nijhoff: Dordrecht, The Netherlands, 1983.

Disclaimer/Publisher's Note: The statements, opinions and data contained in all publications are solely those of the individual author(s) and contributor(s) and not of MDPI and/or the editor(s). MDPI and/or the editor(s) disclaim responsibility for any injury to people or property resulting from any ideas, methods, instructions or products referred to in the content.